Highlights:

- insight into geomorphological processes operating on rocky shores in High Arctic

- first use of SilverSHRT and TMEM tests in Svalbard rocky coast geomorphology study

- geophysical (ERT) evidence of the impact of sea on the state of coastal permafrost

- new conceptual model of High Arctic rock coast system

Cryo-conditioned rocky coast systems: a case study from Wilczekodden, Svalbard

Strzelecki M.C.[1], Kasprzak M.[1], Lim M.[2], Swirad Z.M.[3],Jaskólski M.[1], Pawłowski Ł.[1], Modzel P[1].
1-Institute of Geography and Regional Development, University of Wrocław, pl. Uniwersytecki 1, 50-137 Wroclaw, Poland
2- Engineering & Environment, Northumbria University, Ellison, Northumberland Road, Newcastle upon Tyne NE1 8ST, UK
3-Department of Geography, Durham University, South Road DH1 3LE, Durham UK

Abstract:

This paper presents the results of an investigation into the processes controlling development of a cryo-conditioned rock coast system in Hornsund, Svalbard. A suite of nested geomorphological and geophysical methods have been applied to characterize the functioning of rock cliffs and shore platforms influenced by lithological control and geomorphic processes driven by polar coast environments. Electrical resistivity tomography (ERT) surveys have been used to investigate permafrost control on rock coast dynamics and reveal the strong interaction with marine processes in High Arctic coastal settings. Schmidt hammer rock tests, demonstrated strong spatial control on the degree of rock weathering (rock strength) along High Arctic rock coasts. Elevation controlled geomorphic zones are identified and linked to distinct processes and mechanisms, transitioning from peak hardness values at the ice foot through the wave and storm dominated scour zones to the lowest values on the cliff tops, where the effects of periglacial weathering dominate. Observations of rock surface change using a traversing micro-erosion meter (TMEM) indicate that significant changes in erosion rates occur at the junction between the shore platform and the cliff toe, where rock erosion is facilitated by frequent wetting and drying and operation of nivation and sea ice processes (formation and melting of snow patches and icefoot complexes). The results are synthesised to propose a new conceptual model of High Arctic rock coast systems, with the aim of contributing towards a unifying concept of cold region landscape evolution and providing direction for future research regarding the state of polar rock coasts.

Keywords: rock coast evolution, periglacial processes, cryo-conditioning; **coastal permafrost, Svalbard, High Arctic**

1. Introduction

Since the beginning of the 21st century periglacial researchers have challenged longstanding theoretical concepts of landscape evolution in cold environments (e.g. Hall *et al*., 2002; André, 2003; Thorn, 2004). André (1999) argued that understanding of periglacial environments has been hidden in a 'smokescreen' of theories dominated by climate-driven geomorphic processes involving frost, snow and ice, which were disconnected from the complex processes that operate in periglacial domains. The application of paraglaciation theory in geomorphological studies has emphasised the need for a deeper appreciation of the role of non-glacial processes in present-day polar and high mountain environments (Ballantyne, 2002; Mercier, 2008; André, 2009; Slaymaker, 2011). Berthling and Etzelmüller (2011) introduced the concept of cryo-conditioning to unify interactions between cryotic surface and subsurface thermal regimes and geomorphic processes in determining cold region landscape evolution. An aspect that remains unexplored is the impact of periglacial and paraglacial processes on the evolution of Arctic coastal zones (Figure 1) and in particular on rocky coastlines (Overduin et al., 2014). It is noteworthy that over three decades ago the lack of a consensus on the efficiency of coastal processes in high latitudes was identified by Trenhaile (1983) and still remains.

In the Arctic, sea ice extent and thickness has been declining by more than 10 % per decade since satellite observations began in 1979 (NASA Earth Observatory). This decrease is lengthening the period in which Arctic coastlines are vulnerable to storms and thermal erosion, potentially increasing rates of coastal erosion (Lantuit et al., 2012). In several parts of the Arctic, accelerated glacier retreat has led to the exposure of new fragile coastal systems, where evolution depends on permafrost-related processes and fluxes of sediments from paraglacially transformed landforms. All these changes are expected to impact coastal morphology, causing increased rates of erosion, extensively modifying near shore sediment

and organic carbon mobilization and transport, and potentially pushing coastal systems across critical geomorphological and ecological thresholds (e.g. Fritz et al., 2017).

Up to 35% of Arctic coastlines are rock-dominated and large parts of community and scientific infrastructure are located along rocky coasts (Forbes *et al.* 2011), but few studies have focused specifically on this environment (see Hansom et al. 2014 for a comprehensive review). Previous and classic works on Arctic rock coasts systems emphasized the role of icefoot (e.g. Jahn, 1961; Dionne, 1973; Nielsen, 1979), snow cover (e.g. Ødegård et al., 1995), sea ice and frost weathering (e.g Trenhaile, 1983; Dionne and Brodeur, 1988; Fournier and Allard, 1992; Guilcher et al., 1994; Lundberg and Lauritzen, 2002; Wagensteen et al., 2007) as key controls of shore platform and cliff face geomorphology in polar settings. More recent studies carried out in Svalbard have focused on detailing the characteristics of rock coast weathering using Schmidt hammer rock tests (Strzelecki, 2011; Strzelecki, 2016). Swirad et al. (2017) analysed rock control on the geometry of northern Hornsund coastline. An important progress in understanding of Svalbard coastal systems was recently made by Kasprzak et al. (2016), who used electrical resistivity tomography (ERT) to demonstrate strong influence of the sea on the coastal permafrost base. Previously, this issue has been often overlooked in Arctic coastal studies or hidden under schemas (e.g. Lachenbruch, 1968; Gold and Lachenbruch, 1973), which cannot be universally applied for diverse Arctic coastal systems.

The overarching aim of this study is to characterise the mechanisms controlling present-day development of rocky coastal zone in High Arctic fjord environment with particular focus on the spatial changes in distribution of coastal permafrost and the degree of rock surface weathering along landforms evolving in various lithologies. In this paper we summarise the results of our recent investigations into cryo-conditioned rock coast systems in Svalbard. We have applied a combination of geomorphological and geophysical methods to identify and characterise the effects of periglacial processes operating on rocky cliffs and shore

platforms and propose a new conceptual model of the functioning of High Arctic rock coast systems.

2. Regional setting

The research was undertaken along the rocky coast of Wilczekodden (76.9964°N; 15.5458°E), a small (approx. 500 × 150 m) cape located in Hornsund between the Rettkvalbogen and Isbjørnhamna embayments (Figure 2).

Due to the warm and humid air masses transported by cyclones and warm West Spitsbergen Current, the climatic conditions in Hornsund (Osuch and Wawrzyniak, 2017). The meteorological data published online at www.glacio-topoclim.org/reports, show that the mean annual air temperature (MAAT) during the period from 1979 to 2014 was −4.0 °C. The warmest month was July, with an average temperature of 4.5 °C, the coldest was March, with an average temperature of −10.4 °C. The mean annual precipitation total was 453 mm, but varied significantly from 230.2 mm in 1987 to 635.9 mm in 1996 (Marsz and Styszyńska, 2013). Snow cover thickness reached ca. 0.7 m on the ice-bounded fjord and 1.5 m in the valleys, and wind-blown snow accumulated to depths of more than 3 m at the foot of the cliffs.

The configuration of an adjacent fjord and bordering mountain ranges produce strong topographic control on local wind patterns. Mountains limit northern and southern air masses, which were responsible for only 5.1 % of total detected winds for 1979–2006. Dominant wind directions were recorded from: east (44.1 %), north-east (17.7 %) and west (12.1 %). Mean wind speed in the area is 5.6 m s^{-1} (Kępski et al., 2013). The length (ca. 30 km) and width (14.5 km at the mouth) of open water in the fjord to the west expose the Wilczekodden to long oceanic waves, whilst dominant eastern winds create short, low wind waves that operate within the inner fjord shore. Glacier calving also creates low-frequency waves that modifies the geomorphology of local gravel-dominated barriers (Zagórski et al., 2015).

118 The main geomorphological processes operating on the local strandflat and valley
119 systems reflect both periglacial weathering of relict coastal and glacial landforms and
120 paraglacial remodelling dominated by slope (e.g. Skolasińska et al., 2016; Hartvich et al., 2017),
121 fluvial (e.g. Owczarek et al., 2014; Wawrzyniak et al., 2017), coastal (e.g. Zagórski et al., 2015;
122 Swirad et al., 2017) and permafrost-related processes (e.g. Kasprzak, 2015; Kasprzak et al.,
123 2016). During the last century, all glaciers in the surrounding area have experienced rapid
124 retreat which accelerated between 2001 and 2010 when it reached ~3 km^2 a^{-1} (Błaszczyk et
125 al., 2013). Until the early 1990's the active layer thickness varied around average, 1 - 1.15 m
126 (Baranowski, 1968; Jahn, 1982; Migała, 1994), and due to the climate warming ground thawing
127 depth has recently exceeded 2 m (Dolnicki et al., 2013). However, the active layer
128 development in Hornsund is strongly dependent on ground lithology and land cover, in
129 addition to summer thermal conditions (Migała et al., 2014). For instance, the thickness of the
130 active layer developed in marine gravels and sands was recorded at 2.3 m in late 1980's (Chmal
131 et al., 1988). Frozen ground conditions are extensive and vary from thick and continuous
132 permafrost in mountainous areas to thin (0–10 m), recently developed in deglaciated valleys
133 and along the coast (e.g. Kasprzak et al., 2016).
134 The north-western part of Hornsund is formed from Precambrian rocks, which are a
135 part of the lower and middle Hecla Hoek succession, overlain by Cambrian and Ordovician
136 rock layers (Smulikowski, 1968). Marbles and schists are present at Wilczekodden (Czerny et
137 al., 1992a). Karczewski et al. (1981b) defined 15 levels of raised marine terraces in the
138 Hornsund area covering the extensive strandflat of SW Spitsbergen. Glacial and periglacial
139 landforms (e.g. outwash plains, moraines, roches moutonnées and pingos) cover a significant
140 part of the north-western Hornsund strandflat.
141 Wilczekodden is a rocky cape covered by a series of uplifted marine terraces, forming
142 distinct levels up to 1-2 m high. The fairly evenly distributed marine terraces are studded with

strongly-weathered rocky outcrops (up to 2 m high) associated with relict skerries. Rocky cliffs are present all around the cape, reaching 6 m high along the western marble coast (Figure 2 F) and up to 3 m high along the eastern shale coast (Figure 2 D). The tip of the cape is covered by a steep staircase of raised gravel-dominated beaches, a remnant of still active glacio-isostatic uplift in the area. Accumulations of marine pebbles are also found in several shallow hollows spread across the cape. They are periodically filled with snowmelt waters. Most uplifted marine sediments are sorted by periglacial processes and forms various types of patterned grounds (circles, stripes). The rest of the cape surface is overlaid by coarse weathered debris often vegetated by dry tundra.

3. Materials and methods

3.1 Mapping coastal permafrost using geophysical methods

Electrical resistivity tomography (ERT) allows identification of ground thermal conditions (e.g. Hauck, 2002; Hauck and Krautblatter, 2007; Lewkowicz et al., 2011).The method is based on the application of an electric current into the ground and measurement of the intensity of electrical resistivity. During ERT the electric current (*I*) is transmitted to the ground through two electrodes and the potential difference (*V*) is measured by a second pair of electrodes. Since the bedrock/ground is not a homogeneous body the measured resistivity, which expresses the ratio of voltage to current (taking into account a coefficient (*k*), dependent upon the configuration of the electrodes), is treated as the apparent resistivity. By traversing ERT measurements along a profile and increasing the spacing between the electrodes multiple measurement points can be collected and arranged in separate horizons.

The geophysical surveys utilised the ARES ERT system (GF Instruments, Brno, Czech Republic). The surveys were conducted between 4th and 7th of August 2015 and consisted of four profile lines (Figure 3).

Along the Wilczekodden main profile (P1, Figure 3; 555 m long) and three shorter transverse profiles (Figure 3: P2-4; 155-315 m long). Measurements along each profile have been conducted at 5 m spacing between electrodes. A Werner-Schlumerger electrode array was used to obtain high quality vertical resolution and depth penetration (Loke, 2000; Milsom, 2003; Reynolds, 2011). The results of apparent resistivity have been subjected to standard geophysical interpretation (inversion) using RES2DINV software (Geotomo, Malaysia). The default smoothness-constrained inversion formula (least squares inversion, initial Damping factor = 0.160, minimum Damping factor = 0.015) has also been applied to the data. As a result, the inversion models have been visualized for 3 iterations using a uniform colour scale.

3 .2 Observations of rock weathering and down-wearing processes

3.2.1 Schmidt hammer rock tests

An electronic N-Type Silver Schmidt Hammer manufactured by Proceq was used in this study. The Schmidt hammer measures the rebound of a spring-loaded mass as it impacts on a rock surface providing an arbitrary measure of rock resistance on a scale with a value range 10-100. Six locations were selected along the Wilczekodden coastline (Figure 4) to encompass both main rock types (schist and marble) and the diverse morphologies (note the differences between the east and west sides of the cape, Figure 2).

At each of the six locations the SHRT readings were taken at five elevations: in the intertidal zone, at the high-water level, cliff toe, cliff face and cliff top (Figure 5). Each test comprised of 25 measurements made at points randomly selected from a *ca.* 0.10 × 0.10 m area. The statistical study by Niedzielski et al. (2009) suggested that this number of readings provides an appropriate accuracy of SHRT in the majority of lithologies.

Measurements were conducted on sunny and warm days when the rock surfaces located within the intertidal zone had dried out. The tests were conducted at least 0.05 m

193 from cracks and rock edges and on lichen-free areas following the methodology of Day and
194 Goudie (1977) and Selby (1980).
195
196 *3.2.2 Traversing Micro-Erosion Meter*
197 Traversing Micro-Erosion Meters (TMEMs) measure erosion caused by mechanical,
198 chemical and biological processes with a high precision positioning system based on oblique
199 coordinates. Over the last 30 years TMEMs have been used successfully to study rock surface
200 down-wearing rates in coastal environments (see Stephenson and Finlayson (2009) for a
201 review). Readings are taken by placing the triangular base of the instrument on three bolts
202 that are permanently fastened to a rock surface. The exact re-positioning of the instrument
203 on bolts is possible since each leg has different ends (flat, trench and pit), which also eliminates
204 instrument horizontal movement. The readings are carried out using an engineering dial gauge
205 that is independent of the triangular base and is moved to a number of set positions across
206 the area between three bolts.
207 TMEM used in this study was designed and manufactured by Albatros Marine
208 Technologies (Palma de Mallorca, Spain). We installed six TMEM stations along two profile
209 lines: TM1-TM3 in marbles and TM4-TM6 in schists (Figure 4). At least 10 readings were
210 collected from each TMEM station, generating reasonable estimates of rates of surface change
211 (Trenhaile and Lakhan, 2011). In each profile, the TMEM stations were installed at three
212 locations: in the intertidal zone, at the cliff toe and cliff top. Damage by sea ice action on the
213 bolts installed in schists (TM4-TM6) prevented sufficient readings of surface change.
214 Therefore, the rates of change observed between 02.08.2015 and 21.07.2016 have been
215 established only from stations TM1-TM3 installed in marbles.
216
217 **4. Results and Discussion**
218

4.1 Geophysical surveys

The ERT surveys have revealed the main geoelectrical features of the Wilczekodden cape (Figure 6). The depth of geoelectrical imaging was dependent on the number of electrodes used and the length of the profiles, which ranged from 26 m for P2 with 9 measurement horizons to 82 m for the P1 with 17 measurement horizons. In each case the highest (upper) horizon of measurement points was located at 2.5 m below the ground surface.

The results indicate large contrasts in the geoelectrical characteristics of the ground (electrical resistivity). In the longitudinal profile along the cape (P1, Figure 6), a zone of high resistivity (ρ > 10 kΩ.m) decreases seaward and the influence of mean sea-level on reducing resistivity values is clearly evident at the cliff edge at the cape's southern point. In all cross-section profiles (P2-P4, Figure 6) the highest resistivity zones (ρ > 10 kΩ.m) were situated up to 10 m below the surface.

In the interior of the cape, distant from the sea, the thickness of the layer characterized by high resistivity increases to 30-40 meters below the ground surface (P3 and P4 in Figure 6). Additionally, P3 revealed an isolated zone of low resistivity ρ < 1 kΩ.m detected near the ground surface (Figure 6). The thin weathering surface and relatively simple geology of the Wilczekodden (schists in the east and marbles in the west) aids interpretation of the thermal state of the ground. High values of resistivity are associated with the presence of permafrost. Various values for resistivity of frozen ground are have been provided by previous studies, dependant on many factors (e.g. moisture content, physical characteristics of the rock), but it is generally assumed that bodies with resistivity ρ > 1 kΩ.m generally indicate ice content (e.g. McGinnis et al., 1973; Larin et al., 1978; Arcone and Delaney, 1988; Rein et al., 2004; Halley et al., 2007), although this value can be of a larger magnitude (MacKay, 1969) and such is taken into account in our interpretation (ρ > 10 kΩ.m).

In Wilczekodden the development of permafrost extends from the cape surface to ca. 40 m below the ground. The permafrost forms a wedge orientated towards the shoreline where the thickness of the permafrost layer is reduced and restricted to elevations above present sea-level. The sea-contact control, related to the thermal influences of water temperature and salinity, has parallels with the findings at other nearby embayments: Steinvika, Hyttevika and Veslebogen by Kasprzak et al. (2016).

The anomaly detected in P3 results from a depression covered with marine pebbles and episodically filled by water, that is likely to disturb the thermal state of the ground by thermoerosion (Figure 6). The measurement resolution, with an upper measurement horizon located at 2.5 m below the surface, did not allow detection of active layer extents.

The ERT measurements have indicated the strong influence of the sea on ground/bedrock thermal characteristics in the coastal zone. In summer, both surface water and groundwater are subjected to rising temperatures and salinity due to fjord water ingress (Węsławski 2011). The interpretation of ERT inversion models demonstrates that in the Hornsund region, proximity to coastal waters restricts the development of permafrost. Despite the dependence on assumptions regarding the lithological, structural and textural properties of the ground, similar interpretations have been made in other periglacial environments (e.g. Mackay, 1972; Seguin et al., 1988; Hauck, 2002; Ishikawa, 2004; Krautblatter and Hauck, 2007; Kneisel et al., 2008; Hilbich et al., 2009; You et al., 2013; Kneisel et al., 2014).

4.3. Rock strength and surface change observations

4.3.1 Schmidt hammer rock tests

Schmidt hammer rock tests showed that the rock strength varies considerably as a function of rock type, location along the coast and vertical location at each site (Figure 7). In all cases

269 the highest and most consistent (lowest error) R-values (65-75) were recorded in the
270 intertidal zone, while the lowest and most variable R-values (30-52) occurred at the cliff top.
271 In general, the marble cliff sites (M1-M3, Figure 7) recorded higher strength (hardness
272 rebound) values, reducing less with elevation and exhibiting lower variability (<20 if cliff top
273 of M3 excluded). Rock hardness is much more diverse for the schist cliff sites (S1-S3), as the
274 R-values do not decrease consistently when moving up the cliff and the standard error remains
275 relatively high (up to 3.8). Site M3 has the most significant (of 45) reduction of hardness values
276 from the intertidal zone to the cliff top.

277 The two rock types of the Wilczekodden respond to weathering and erosive
278 processes differently. At the marble cliff sites, the rock strength and hardness consistency
279 decrease systematically landwards from the intertidal zone. In contrast, at the schist cliff sites
280 the R-value distribution is not consistent between cross-profiles. The discrepancy may be due
281 to differences in micro-structure of the two rock types, where marble is more massive and
282 schist is composed of thin layers with strong orientation control (Swirad et al., 2017). In
283 general, rock strength is the lowest on the cliff top where wave action is absent and
284 weathering due to nivation, freeze-thaw and wet-dry cycles is intense.

285 The strength of the rock surface depends on the intact rock mass strength (directly
286 linked with rock type and structure) and deterioration due to weathering (Selby, 1980). Chelli
287 et al., (2010) noticed that in coastal settings the strength depends on both the type of rock
288 and mechanical weathering (wetting/drying cycle).

289 Along the Wilczekodden the level of weathering due to wetting and drying varies
290 considerably in relation to tidal inundation and patterns of wave action. In periglacial
291 environments further process control is exerted by the presence and movement of sea ice,
292 the formation of an icefoot, partial snow cover and freeze-thaw weathering (e.g. Trenhaile,
293 1997; Hansom et al., 2014; Strzelecki, 2016).

294 In the intertidal zone the rock surface is eroded by wave and sea ice action, removing the
295 weathering surface (Blanco-Chao et al., 2007) and leading to higher and more repeatable
296 (consistent) Schmidt hammer reading in this zone (Williams and Robinson, 1983; Goudie,
297 2006). The increasing weathering influence with elevation above sea-level is similar to patterns
298 observed on sandstone and anhydrite cliffs in Billefjorden, central Spitsbergen (Strzelecki,
299 2016).
300
301 *4.3.2 Traversing micro-erosion meter measurements*
302 The average surface change at each station has been derived by calculating the total
303 erosion/swelling present at each measurement point and dividing by the number of points.
304 Over the study period, the stations experienced surface change at different rates according
305 to their elevation. The down-wearing of the rock surface was observed only at station TM2
306 installed at the cliff toe (mean surface vertical erosion -1.2 mm). At the top of the cliff (TM1,
307 Figure 8) the surface remained unchanged, whereas surface swelling was observed at station
308 TM3 installed in the intertidal zone (mean surface elevation 0.2 mm).
309 Although limited to one profile, these observations demonstrate that micro-erosion
310 occurred only at coastal elevations subject to wave impacts and to the most frequent and
311 complete shifts in wetting and drying where wetting from tides, waves and spray are often
312 completely dried out before rewetting. The swelling observed on the surface of shore
313 platform is a relatively common process associated with crystallization of salt, algae growth,
314 heating and cooling as well as wetting and drying (Stephenson and Finlayson, 2009).
315 In High Arctic settings, such as Svalbard, the remaining question is the role of
316 stagnation and melting of sea-ice floes on the surface of shore platforms leading to significant
317 cooling of rock surfaces regardless of daytime heating. Values of rock surface swelling

318 observed in Wilczekodden were similar to those from other morphoclimatic sites (e.g.
319 Stephenson and Kirk 2001; Trenhaile, 2006).
320
321 *4.4 Implications for the conceptual model of a High Arctic rock coast system*
322 In order to develop a general model of cryo-conditioned rocky coast zones developing
323 in polar regions, a schematic summary of the dominant processes is presented in Figure 9.
324 Based on the observations of rocky shores forming along Wilczekodden and results of
325 previous rock coast studies in Svalbard (e.g. Jahn, 1961; Ødegård and Sollid, 1993; Ødegård
326 et al., 1995; Migoń, 1997; Wangensteen et al., 2007; Strzelecki, 2011; Kasprzak et al., 2016;
327 Strzelecki 2016; Swirad et al., 2017), the rocky coast system has been divided into seven
328 geomorphic zones (Table 1).
329 The evolution of High Arctic rocky coasts is associated with seasonal variability in sea
330 ice action, frost weathering, permafrost-dependent rock saturation and snow insulation
331 (Trenhaile and Mercan, 1984; Dawson et al., 1987). Strzelecki (2016) highlighted the role of
332 debris cover and bioagents (driftwood, seaweeds, birds) in shaping cold region rocky cliff and
333 platform morphology.
334 High Artic coastal regions are also characterised by microtides and reduced wave
335 action due to sea ice cover. Therefore, it is possible to isolate the relative importance of rock
336 resistance and wave-, tide- and frost-induced processes on coastal morphology.
337 The two existing models of periglacial shore platform evolution proposed by Hansom
338 (1983) for South Shetland Islands, Antarctica and Fournier and Allard (1992) for Ungava Bay,
339 Arctic envisage rapid adjustment of coastlines, partially inherited from former sea high stands
340 to the present morphoclimatic environment.
341 A somewhat different situation may exist along High Arctic coastlines, which have
342 been exposed to coastal processes for the first time during the Holocene. In these settings,

coastal evolution is strongly influenced by post-glacial rock debuttressing, the rate of land uplift and relative sea-level changes. Many High Arctic archipelagos such as Svalbard, the Canadian Arctic Archipelago, Franz Josef Land, Novaya Zemlya have experienced rapid coastal emergence or submergence related glacio-isostatic adjustment to deglaciation and associated with relative sea-level (RSL) changes (e.g. Forman et al., 2004; Long et al., 2012). Therefore, High Arctic rocky coastlines provide an excellent test area for various hypotheses in shore platform development in periglacial conditions as yet described mainly on lacustrine examples from Scotland (Sissons, 1978; Dawson, 1980), Norway (Matthews et.al, 1986; Dawson et al., 1987; Shakesby and Matthews, 1987; Aarseth and Fosgen, 2004) and Canada (Trenhaile, 2004). The well-dated chronology of RSL change based on widespread uplifted beaches provides a useful basis for exploration of the time-dependence of cliff and platform evolution, as well as the operation of geomorphic processes. For instance, the development of coastal karst dolina relief in Vardeborgsletta, characteristic for carbonate and evaporite outcrops in central and eastern Spitsbergen, has been strongly linked with sea-level change (Salvigsen and Elgersma, 1985). Karstic processes in rocky coasts are likely to have been initiated during Holocene sea-level highstands, when frozen rocks thawed and subsequently emerged due to rapid glacioisostatic uplift. More recently a novel study by Hanken et al. (2012) indicated that the presence of polychaete borings in subaerially exposed bedrock surfaces can be used to evaluate postglacial emergence on Svalbard in the absence of well-preserved uplifted beach sediments or isolation basins.

5. Conclusions

For the first time in the High Arctic setting the rock coast system has been investigated using the combination of geomorphological (SHRT, TMEM) and geophysical (ERT) methods. Based on the observations we have drawn the following conclusions:

1. The development of permafrost along Wilczekodden rocky coast is controlled by the thermal influence of sea water. Coastal permafrost evolves in the form of a wedge directed towards the shoreline.
2. Rock surface strength across shore platforms and cliffs depends on the efficiency of processes removing weathered and eroded material. In both tested lithologies (marbles and schists), the lowest rock strengths were observed along the top of the cliffs, subject primarily to periglacial weathering, whereas erosional processes operating across shore platforms and cliff bases lead to exposure of fresh and resistant rock surfaces.
3. For the first time in Hornsund, we have analysed the changes of rock surfaces using a traversing micro-erosion meter. Significant differences exist in the behaviour of rock surfaces located at the cliff top, cliff toe, and in the intertidal zone. Surface down-wearing occurred only at the base of the cliff exposed to frequent wetting and drying, storm wave impact and changes of thickness, duration and degradation of snowpatches and icefoot complexes.
4. Future research in High Arctic settings should include the role of processes associated with the frost and ice action. In addition, it is important that future studies consider: the spatial distribution of permafrost; the significance of diurnal and annual freeze-thaw cycles modified by wetting and drying; the influence of reduced icefoot size on the rock cliff and platform evolution; the climate-driven incorporation of debris from cliff abrasion into sea ice; type of bioagents operating on coastal rock surface, and finally, the impact of recently delivered paraglacial sediments on erosion or protection of rocky shorelines.

Acknowledgements:

This is a contribution to the National Science Centre project UMO2013/11/B/ST10/00283: ' POROCO – Mechanisms controlling the evolution and geomorphology of rock coasts in polar climates'. Matt Strzelecki is supported by NCN Postdoctoral Fellowship FUGA and the Ministry of Science and Higher Education Outstanding Young Scientist Scholarship. The author thanks the participants of 11th International Conference on Permafrost their constructive comments on the results presented in this study. We thank reviewers Professor Alan Trenhaile and Filip Hrbacek, and the Editor for their very thoughtful and constructive comments, which significantly improved the manuscript. This research is a contribution to the IAG Sediment Budgets in Cold Environments Working Group.

405 **References:**

406 Aarseth, I., Fosgen H., 2004. A Holocene lacustrine rock platform around Storavatnet,
407 Osterøy, western Norway. Holocene 14: 589-596.
408 André, M-F., 1999. La livrée périglaciaire des paysages polaires: l'arbre qui cache la forêt? The
409 periglacial scenery of polar areas: a smoke-screen? Géomorphologie: relief, processus,
410 environnement 5: 231 – 251.
411 André, M-F., 2003. Do periglacial landscapes evolve under periglacial conditions?
412 Geomorphology 52: 149-164.
413 André, M-F., 2009. From climatic to global change geomorphology: contemporary shifts in
414 periglacial geomorphology. In Knight J., and Harrison S., (Eds.) Periglacial and Paraglacial
415 Processes and Environments. Geological Society, London Special Publications 320: 5-28.
416 Arcone, S.A., Delaney, A.J., 1988. Borehole investigations of the electrical properties of frozen
417 silt. In: Senneset, K. (Ed.), Permafrost. Fifth International Conference. August 2–5,
418 Proceedings Volume 2, Tapir Pub., Trondheim, Norway, pp. 910–915.
419 Ballantyne, C., 2002. Paraglacial geomorphology. Quaternary Science Reviews 21: 1935–2017.
420 Baranowski, S. 1968. Thermic conditions of the periglacial tundra in SW Spitsbergen. Acta
421 Universitas Wratislaviensis 68: 74 pp.
422 Berthling, I., Etzelmüller B., 2011. The concept of cryo-conditioning in landscape evolution.
423 Quaternary Research 75: 378-384.
424 Blanco-Chao, R., Pérez-Alberti, A., Trenhaile, A.S., Costa-Casais, M., Valcárcel-Díaz, M., 2007.
425 Shore platform abrasion in a para-periglacial environment, Galicia, northwestern Spain.
426 Geomorphology 83: 136–151.
427 Błaszczyk, M., Jania, J., Kolondra, L., 2013. Fluctuations of tidewater glaciers in Hornsund Fjord
428 (Southern Svalbard) since the beginning of the 20th century. Polish Polar Research 34: 327-
429 352.

Byrne, M-L., Dionne, J-C., 2002. Typical Aspects of Cold regions Shorelines. In: Hewitt K., Byrne M-L., English M., Young G., (Eds.), Landscapes in Transition. Landform Assembladges and Transformations in Cold Regions. Kluver Academic Publishers, Dordrecht: 141- 158.

Chelli, A., Pappalardo, M., Llopis, I.A., Federici, P. B., 2010. The relative influence of lithology and weathering in shaping shore platforms along the coastline of the Gulf of La Spezia (NW Italy) as revealed by rock strength. Geomorphology 118: 93-104.

Chmal, H., Klementowski, J., Migała, K., 1988. Thermal currents of active layer in Hornsund area. In: Senneset, K. (Ed.), Permafrost. Fifth International Conference. August 2–5, Proceedings Volume 1, Tapir Pub., Trondheim, Norway, pp. 44–49.

Czerny, J., Kieres, A., Manecki, M., Rajchel, J., 1992. Geological Map of the SW Part of Wedel Jarlsberg Land Spitsbergen, 1:25 000. Institute of Geology and Mineral Deposits, Univ. of Mining and Metallurgy, Cracow.

Davies, J. L., 1980. Geographical Variation in Coastal Development. London: Longman Group Ltd., 212p.

Dawson, A. G., Matthews, J. A., Shakesby, R. A., 1987. Rock platform erosion on periglacial shores: a modem analogue for Pleistocene rock platforms in Britain. In Boardman, J. (ed.): Periglacial processes and landforms in Britain and Ire/and. Cambridge University Press, Cambridge 173--182.

Day, M.J., and Goudie, A.S., 1977. Field assessment of rock hardness using the Schmidt test hammer. British Geomorphology Research Group Technical Bulletin 18: 19–29.

Dickson, M.E., Kennedy, D.M., Woodroffe, C.D., 2004. The influence of rock resistance on coastal morphology around Lord Howe Island, Soutwest Pacific. Earth Surface Processes and Landforms 29: 629–643.

Dionne, J.-C., 1973. La motion de pied de glace (Ice-foot), en particulier dans l'estuaire du Saint-Laurent, Cahiers Géographie Québec 17: 221–250.

455 Dionne, J.-C., Brodeur, D., 1988. Frost weathering and ice action in shore platform
456 development, with particular reference to Quebec, Canada. Zeitschrift für
457 Geomorphologie Supplement band 71: 117-30.
458 Dolnicki, P., Grabiec, M., Puczko, D., Gawor, Ł., Budzik, T., Klementowski, J., 2013. Variability
459 of temperature and thickness of permafrost active layer at coastal sites of Svalbard. Polish
460 Polar Research 34: 353–374.
461 Forbes, D.L. (editor), 2011. State of the Arctic Coast 2010 – Scientific Review and Outlook.
462 International Arctic Science Committee, Land-Ocean Interactions in the Coastal Zone,
463 Arctic Monitoring and Assessment Programme, International Permafrost Association.
464 Helmholtz-Zentrum, Geesthacht, Germany: 178; http://arcticcoasts.org
465 Forman, S., Lubinski, D., Ingolfsson, O., Zeeberg, J., Snyder, J., Siegert, M., Matishov, G., 2004.
466 A review of postglacial emergence on Svalbard, Franz Josef Land and Novaya Zemlya,
467 northern Eurasia. Quaternary Science Reviews 23: 1391–1434.
468 Fournier, A., Allard, M., 1992. Periglacial shoreline erosion of rocky coast: George River
469 Estuary, Northern Quebec. Journal of Coastal Research 8: 926-942.
470 Fritz, M., Vonk, J.E., Lantuit, H., 2017. Collapsing Arctic coastlines. Nature Climate Change 7,
471 6-7. http://dx.doi.org/10.1038/nclimate3188.
472 Gold, L.W., Lachenbruch, A.H., 1973. Thermal conditions in permafrost – a review of North
473 American literature. In: Permafrost Second International Conference, 13–28 July 1973,
474 Yakutsk, U.S.R.R., North American Contribution, Arlis, National Academy of Sciences,
475 Washington, pp. 3–25.
476 Goudie, A., 2006. The Schmidt Hammer in geomorphological research. Progress in Physical
477 Geography 30: 703–718.

478 Guilcher, A., Bodere, J.-C., Coude, A., Hansom, J. D., Moign, A. and Peullvast, J.-P. (1994) The
479 Strandflat problem in five high latitude countries. In: Evans, D. J.A. (ed.) Cold Climate
480 Landforms. Wiley: Chichester, pp. 351-393.
481 Hall, K., Thorn, C., Matsuoka, N., Prick, A., 2002. Weathering in cold regions.: Some thoughts
482 and perspectives. Progress in Physical Geography 4: 576-602.
483 Halley, K., Bentley, L.R., Gharibi, M., Nightingale, M., 2007. Low temperature dependence of
484 electrical resistivity: Implications for near surface geophysical monitoring. Geophysical
485 Research Letters 34, L18402, doi:10.1029/2007GL031124
486 Hanken N-M., Uchman, A., Jakobsen , S.L., 2012. Late Pleistocene-early Holocene polychaete
487 borings in NE Spitsbergen and their palaeoecological and climatic implications: an example
488 from the Basissletta area. Boreas 41: 42-55.
489 Hansom, J.D., 1983. Shore-platform development in the South Shetland Islands, Antarctica.
490 Marine Geology 53: 211-229.
491 Hansom, J.D., Forbes, D.L., Etienne, S., 2014. The rock coasts of polar and sub-polar regions.
492 In Kennedy D. M., Stephenson W. J. & Naylor L. A. (Eds) 2014. Rock Coast
493 Geomorphology: A Global Synthesis. Geological Society, London, Memoirs, 40: 263–281.
494 Hartvich, F., Blahut, J., Stemberk, J., 2017. Rock avalanche and rock glacier: A compound
495 landform study from Hornsund, Svalbard. Geomorphology 276: 244-256.
496 Hauck, C. 2002. Frozen ground monitoring using DC resistivity tomography. Geophysical
497 Research Letters 29(21): 2016, doi:10.1029/2002GL014995
498 Hilbich, C., Marescot, L., Hauck, C., Loke, M.H., Mäusbacher, R., 2009. Applicability of
499 Electrical Resistivity Tomography Monitoring to Coarse Blocky and Ice-rich Permafrost
500 Landforms. Permafrost and Periglacial Processes 20: 269–284.
501 Ishikawa, M., 2004, Application of DC resistivity imaging to frozen ground investigations.
502 Journal of the Japanese Society of Snow and Ice 66: 177–186.

503 Jahn, A., 1961. Quantitative analysis of some periglacial processes in Spitsbergen. Zeszyty
504 Naukowe Uniwersytetu Wrocławskiego Seria B, nr 5, Geophysics, Geography, Geology II:
505 3-54.
506 Jahn, A. 1982. Soil thawing and active layer of permafrost in Spitsbergen. Acta Universitatis
507 Wratislaviensis 525, Spitsbergen Expeditions IV, pp. 57–75.
508 Kasprzak, M., 2015. High-resolution electrical resistivity tomography applied to patterned
509 ground, Wedel Jarlsberg Land, south-west Spitsbergen. Polar Research 34(25678): 1-13.
510 Kasprzak, M., Strzelecki, M.C., Traczyk, A., Kondracka, M., Lim, M., Migała, K., 2016. On the
511 potential for a bottom active layer below coastal permafrost: the impact of seawater on
512 permafrost degradation imaged by electrical resistivity tomography (Hornsund, SW
513 Spitsbergen). Geomorphology, http://dx.doi.org/10.1016/j.geomorph.2016.06.01
514 Kępski, D., Górski, Z., Benedyk, M., Szumny, M., Wawrzyniak, T., 2013. Meteorological
515 bulletin. Spitsbergen-Hornsund. Summary of the year 2-13. Polish Polar Station, Institute
516 of Geophysics, Polish Academy of Sciences.
517 Kneisel, C., Hauck, C., Fortier, R., Moorman, B., 2008. Advances in geophysical methods for
518 permafrost investigations. Permafrost and Periglacial Processes 19: 157–178.
519 Kneisel C., Emmert, A., Kästl, J., 2014. Application of 3D electrical resistivity imaging for
520 mapping frozen ground conditions exemplified by three case studies. Geomorphology 210:
521 71–82.
522 Krautblatter M. & Hauck C. 2007. Electrical resistivity tomography monitoring of permafrost
523 in solid rock walls. Journal of Geophysical Research: Earth Surface 112, F2, 2156–2202.
524 Lachenbruch, A.H. 1968. Permafrost. In: Fairbridge, R.W. (Ed.), The encyclopedia of
525 geomorphology. New York, Reinhold Pub. Corp., pp. 833–839.
526 Lantuit, H., Overduin, P.P., Couture, N., Wetterich, S., Are, F., Atkinson, D., Brown, J.,
527 Cherkashov, G., Drozdov, D., Forbes, D.L., Graves-Gaylord, A., Grigoriev, M., Hubberten,
528 H.W., Jordan, J., Jorgenson, T., Ødegård, R.S., Ogorodov, S., Pollard, W., Rachold, V.,

529 Sedenko, S., Solomon, S., Steenhuisen, F., Streletskaya, I., Vasiliev, A., 2012. The Arctic
530 Coastal Dynamics database. A new classification scheme and statistics on Arctic permafrost
531 coastlines. Estuaries and Coasts 35: 383-400.
532 Larin, S.M., Marov, G.P., Kholmyanskiy, M.A., Neizvestnov, Ya.V., 1978. Certain types of
533 geoelectric sections of the negative temperature belt in the arctic and subarctic connection
534 with exploration for subpermafrost. In: Sanger, F.J, Hyde, P.J. (Eds), Permafrost Second
535 International Conference, 13–28 July 1973, Yakutsk, U.S.R.R., USRR Contribution, National
536 Academy of Sciences, Washington, pp. 428–430.
537 Lewkowicz A.G., Etzelmüller B. & Smith S.L. 2011. Characteristics of discontinuous
538 permafrost based on ground temperature measurements and electrical resistivity
539 tomography, Southern Yukon, Canada. Permafrost and Periglacial Processes 22 320–342.
540 Loke, M.H. 2000. Electrical imaging syrveys for environmental and engineering studies. A
541 practical guide to 2-D and 3-D surveys. Geotomo, Malaysia.
542 Long, A.J., Strzelecki, M.C., Lloyd, J.M., Bryant, C., 2012. Dating High Arctic Holocene relative
543 sea level changes using juvenile articulated marine shells in raised beaches. Quaternary
544 Science Reviews 48: 61-66.
545 Lundberg, J., Lauritzen, S-E., 2002. The search for an Arctic coastal karren model in Norway
546 and Spitzbergen. In: Hewitt K., Byrne M-L., English M. and Young G., (Eds.), Landscapes in
547 Transition. Landform Assembladges and Transformations in Cold Regions. Kluver
548 Academic Publishers, Dordrecht: 185-203.
549 MacKay, D.K., 1969. Electrical resistivity measurements in frozen ground, Mackenzie Delta
550 area, Northwest Territories. Association Internationale d'Hydrologie Scientifique, Actes
551 du Colloque de Becarest, Reprint Ser. 82, Department of Energy, Mines and Resources,
552 Inland Waters Branch, Ceuterick, Belgium, pp. 363–375.
553 Mackay, J.R., 1972. Offshore permafrost and ground ice, Southern Beaufort Sea, Canada.
554 Canadian Journal of Earth Sciences 9(11), 1550–1561.
555 Marsz, A.A., Styszyńska, A. (Eds.). 2013. Climate and Climate Change at Hornsund, Svalbard.
556 Authors: J. Ferdynus, A.A. Marsz, A. Styszyńska - Gdynia Martitime University, E. Łupikasza,

557 T. Niedźwiedź - University of Silesia). The publishing house of Gdynia Maritime University,
558 Gdynia, 402 p.
559 Matthews, J., Dawson, A.G., Shakesby, R.A. 1986: Lake shoreline development, frost
560 weathering and rock platform erosion in an alpine periglacial environment, Jotunheimen,
561 southern Norway. Boreas 15: 33-50.
562 McGinnis, L.D., Nakao, K., Clark, C.C., 1973, Geophysical identification of frozen and
563 unfrozen ground, Antarctica. In: Permafrost Second International Conference, 13–28 July
564 1973, Yakutsk, U.S.R.R., North American Contribution, Arlis, National Academy of
565 Sciences, Washington, pp. 3–25.
566 Mercier, D., 2008. Paraglacial and paraperiglacial landsystems: concepts, temporal scales and
567 spatial distribution. Géomorphologie: relief, processus, environnement 4: 223-234.
568 Migała, K., 1994. The characteristic features of the active layer of the permafrost in the climate
569 of Spitsbergen (in Polish with Eng. abstract). Acta Universitatis Wratislaviensis 1590 (Prace
570 Instytutu Geograficznego C, Meteorologia i Klimatologia) 1, 79–111.
571 Migała, K., Wojtuń, B., Szymański, W., Muskała, P., 2014. Soil moisture and temperature
572 variation under different types of tundra vegetation during the growing season: A case
573 study from the Fuglebekken catchment, SW Spitsbergen. Catena 116, 10–18.
574 Migoń, P., 1997. Post−emergence modification of marine cliffs and associated shore platforms
575 in periglacial environment, SW Spitsbergen: implications for the efficacy of cryoplanation
576 processes. Quaternary Newsletter 81: 9–17.
577 Milsom, J., 2003. Resistivity methods. In: Field Geophysics 3rd Edition. Wiley, Chichester. 97–
578 116.
579 Niedzielski, T., Migoń, P., Placek, A., 2009. A minimum sample size required for Schmidt
580 Hammer measurements. Earth Surface Processes and Landforms 34: 1713–1725.

581 Nielsen, N., 1979. Ice-foot processes. Observations of erosion of the rocky coast, Disko,
582 West Greenland. Zeitschrift für Geomorphologie 23: 321-331.
583 Ødegård, R. S., Sollid J.L., 1993. Coastal cliff temperatures related to the potential for
584 cryogenic weathering processes, western Spitsbergen, Svalbard. Polar Research 12: 95-106.
585 Ødegård, R. S, Etzelmüller, B., Vatne G., Sollid J., 1995. Nearsurface spring temperatures in
586 an Arctic coastal cliff: possible implications of rock breakdown. In SLAYMAKER O. (Ed.):
587 Steepland geomorphology. Wiley, Chichester UK: 89–102. Osuch, M., Wawrzyniak, T.,
588 2017. Inter- and intra-annual changes in air temperature and precipitation in western
589 Spitsbergen. International Journal of Climatology 37: 3082–3097.
590 Overduin, P.P., Strzelecki, M.C., Grigoriev, M.N., Couture, N., Lantuit, H., St-Hilaire-Gravel
591 D., Günther, F., Wetterich, S., 2014. Coastal changes in the Arctic. In: Martini, I. P.,
592 Wanless, H. R. (eds.) Sedimentary Coastal Zones from High to Low Latitudes: Similarities
593 and Differences. Geological Society, London, Special Publications, 388: 103-129.
594 Owczarek, P., Nawrot, A., Migała, K., Malik, I., Korabiewski, B., 2014. Flood-plain
595 responses to contemporary climate change in small High-Arctic basins (Svalbard,
596 Norway). Boreas 43: 384–402.
597 Rein, A., Hoffmann, R., Dietrich, P., 2004. Influence of natural time- dependent variations of
598 electrical conductivity on DC resistivity measurements. Journal of Hydrology 285: 215–
599 232.
600 Reynolds, J.M., 2011. Electrical Resistivity Methods. In: An Introduction to Applied and
601 Environmental Geophysics. 2nd Ed., Wiley, Chichester, pp. 289–372.
602 Salvigsen, O., Elgersma, A., 1985. Large-scale karst features and open taliks at Vardeborgsletta,
603 outer Isfjorden, Svalbard. Polar Research 3: 145—153.
604 Seguin, M.K., Gahe, E., Allard, M., Ben-Mikoud, K. 1988. Permafrost geophysical investigation
605 at the new airport site of Kangiqsualujjuaq, Northern Quebec, Canada. In: Senneset, K.

606 (Ed.), Permafrost. Fifth International Conference. August 2–5, Proceedings Volume 2, Tapir
607 Pub., Trondheim, Norway, pp. 980–987.
608 Selby, M.J., 1980. A rock mass strength classification for geomorphic purposes: with test from
609 Antarctica and New Zealand. Zeitschrift für Geomorphologie 24: 31–51.
610 Shakesby, R.A., Matthews, J.A., 1987. Frost weathering and rock platform erosion on
611 periglacial lake shorelines: a test of a hypothesis. Norsk Geologisk Tidsskrift 67: 197-203.
612 Sissons, J.B., 1978. The parallel roads of Glen Roy and adjacent glens, Scotland. Boreas 7: 229-
613 44.
614 Skolasińska K., Rachlewicz G., Szczuciński W., 2016. Micromorphology of modern tills in
615 southwestern Spitsbergen - Insights into depositional and post-depositional processes.
616 Polish Polar Research 37: 435-456.
617 Slaymaker, O., 2011. Criteria to distinguish between periglacial, proglacial and paraglacial
618 environments. Quaestiones Geographicae 30: 85–94.
619 Smulikowski, W. (1968): Some petrological and structural observations in the Hecla Hoek
620 succession between Werenskioldbreen and Torelbreen, Vestspitsbergen. Studia
621 Geologica Polonica 21: 97-161.
622 Stephenson, W.J., Kirk, R.M., 2001. Surface swelling of coastal bedrock on inter-tidal shore
623 platforms, Kaikoura Peninsula, South Island, New Zealand. Geomorphology 41: 5-21.
624 Stephenson, W.J., Finlayson, B.L., 2009. Measuring erosion with the micro-erosion meter–
625 contributions to understanding landform evolution. Earth Science Reviews 95:53–62.
626 Strzelecki, M.C., 2011. Schmidt hammer tests across recently deglacierized rocky coastal zone
627 – is there a 'coastal amplification' of rock weathering in polar climates? Polish Polar
628 Research 32: 239-252.
629 Strzelecki, M.C., 2016, The variability and controls of rock strength along rocky coasts of
630 central Spitsbergen, High Arctic. Geomorphology, doi: 10.1016/j.geomorph.2016.06.014

631 Swirad, Z.M., Migoń, P., and Strzelecki, M.C., 2017. Rock control on the geometry of coastal
632 embayments of north-western Hornsund, Svalbard, Zeitschrift für Geomorphologie 61(1):
633 11-28.
634 Thorn, C., 2004. Whither, or wither, periglacial weathering studies? Polar Geography 28: 4-
635 12.
636 Trenhaile, A.S., 1983. The development of shore platforms in high latitudes. In: D.E. Smith and
637 A.G. Dawson (eds.), Shorelines and Isostasy. Institute of British Geographers, Special
638 publication No. 16, London: 77-96.
639 Trenhaile, AS. 1997. Coastal Dynamics and Landforms. Oxford University Press, Oxford, UK,
640 pp.366.
641 Trenhaile, A.S., 2002. Modeling the effect of weathering on the evolution and morphology of
642 shore platforms. Journal of Coastal Research 17: 398–406.
643 Trenhaile, A.S., 2004. Lacustrine shore platforms in southwestern Ontario, Canada. Zeitschrift
644 für Geomorphologie 48: 441-459.
645 Trenhaile, A.S., 2006. Tidal wetting and drying on shore platforms: An experimental study of
646 surface expansion and contraction. Geomorphology 76: 316-331.
647 Trenhaile, A.S., Mercan, D.W., 1984. Frost weathering and the saturation of coastal rocks.
648 Earth Surface Processes and Landforms 9: 321–331.
649 Trenhaile, A.S., Lakhan, V.C., 2011. Transverse micro-erosion meter measurements;
650 determining minimum sample size. Geomorphology 134: 431–439
651 Trenhaile, A.S., Perez Alberti, A., Martınez Cortizas, A., Costa-Casais, M., Blanco Chao, R.,
652 1999. Rock coast inheritance: an example from Galicia, Northwestern Spain. Earth Surface
653 Processes and Landforms 24: 1 – 17.

Viles, H., Goudie, A., Grab, S., Lalley, J., 2011. The use of the Schmidt Hammer and Equotip for rock hardness assessment in geomorphology and heritage science: a comparative analysis. Earth Surface Processes and Landforms 36: 320-333.

Wangensteen, B., Eiken, T., Ødegård, R.S., Sollid, J.L., 2007. Measuring coastal cliff retreat in the Kongsfjorden area, Svalbard, using terrestrial photogrammetry. Polar Research 26: 14–21.

Wawrzyniak, T., Osuch, M., Nawrot, A., Napiorkowski, J. 2017. Run-off modelling in an Arctic unglaciated catchment (Fuglebekken, Spitsbergen). Annals of Glaciology, 1-11. doi:10.1017/aog.2017.8

Węsławski, J.M. (ed.), 2011. Adventfjorden. Arctic sea in the backyard. Institute of Oceanology PAS, Sopot, pp. 39.

Williams, R. B. G., Robinson, D. A., 1983. The effect of surface texture on the determination of the surface hardness of rock using the schmidt hammer. Earth Surface Processes and Landforms 8: 289–292.

You, Y., Yu, Q., Pan, X., Wang, X., Guo, L. 2013. Application of electrical resistivity tomography in investigating depth of permafrost base and permafrost structure in Tibetan Plateau. Cold Regions Science and Technology 87, 19–26. 35.

Zagórski, P., Rodzik, J., Moskalik, M., Strzelecki, M.C., Lim, M., Błaszczyk, M., Promińska, A., Kruszewski, G.,2015. Multidecadal (1960–2011) shoreline changes in Isbjørnhamna (Hornsund, Svalbard). Polish Polar Research 36: 369–390.

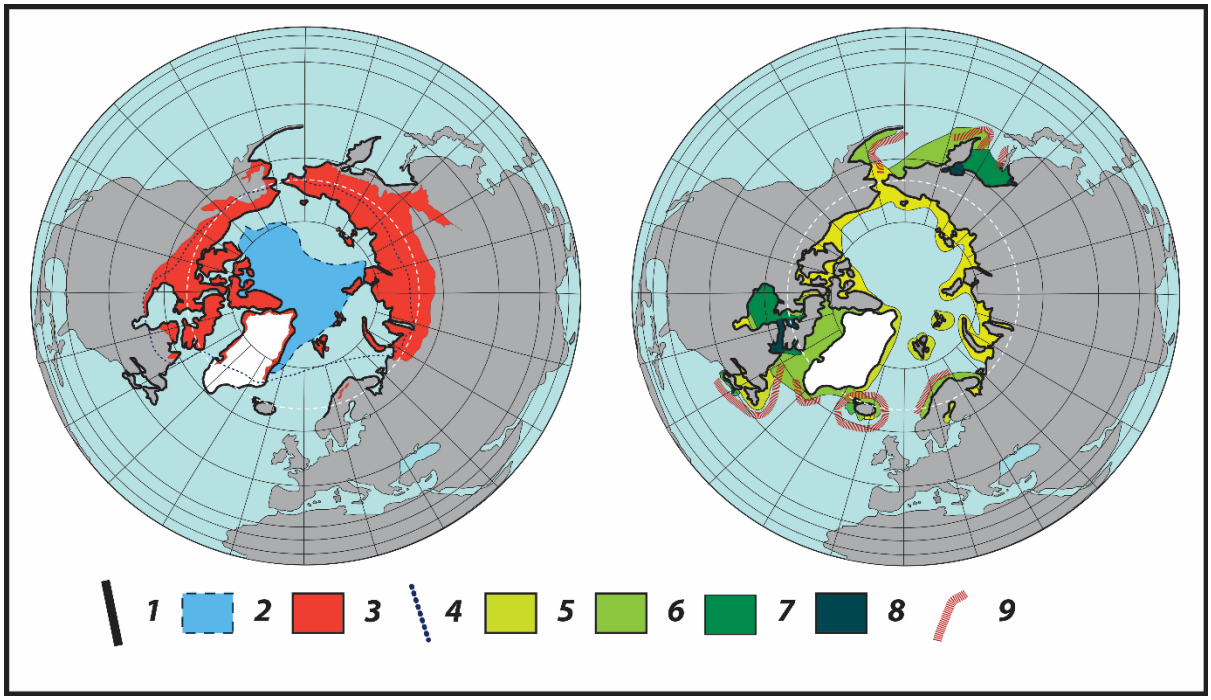

Figure 1. Regional climatic and oceanographic factors controlling Arctic coastal geomorphology predicted to alter due to global warming and sea-level rise. 1 - cold region coasts according to Byrne and Dionne (2002) – defined as 'areas where frost and ice processes are active during a period of the year, which is sufficient to have a significant, if not permanent, impact on the near terrestrial, coastal and marine environments'; 2 – minimum arctic sea ice extent in August 2016 (source: National Snow and Ice Data Centre: http://nsidc.org/); 3 - zone of continuous permafrost (source: National Snow and Ice Data Centre: http://nsidc.org/); 4 – zone of less than 60 frost-free days per year (after Davies 1980); Spring tidal range along cold region coasts (after Davies 1980): 5 – tides <2 m; 6 – tides 2-4 m; 7 – tides 4-6 m; 8 – tides >6 m; 9 – storm wave environments in cold regions (after Davies, 1980).

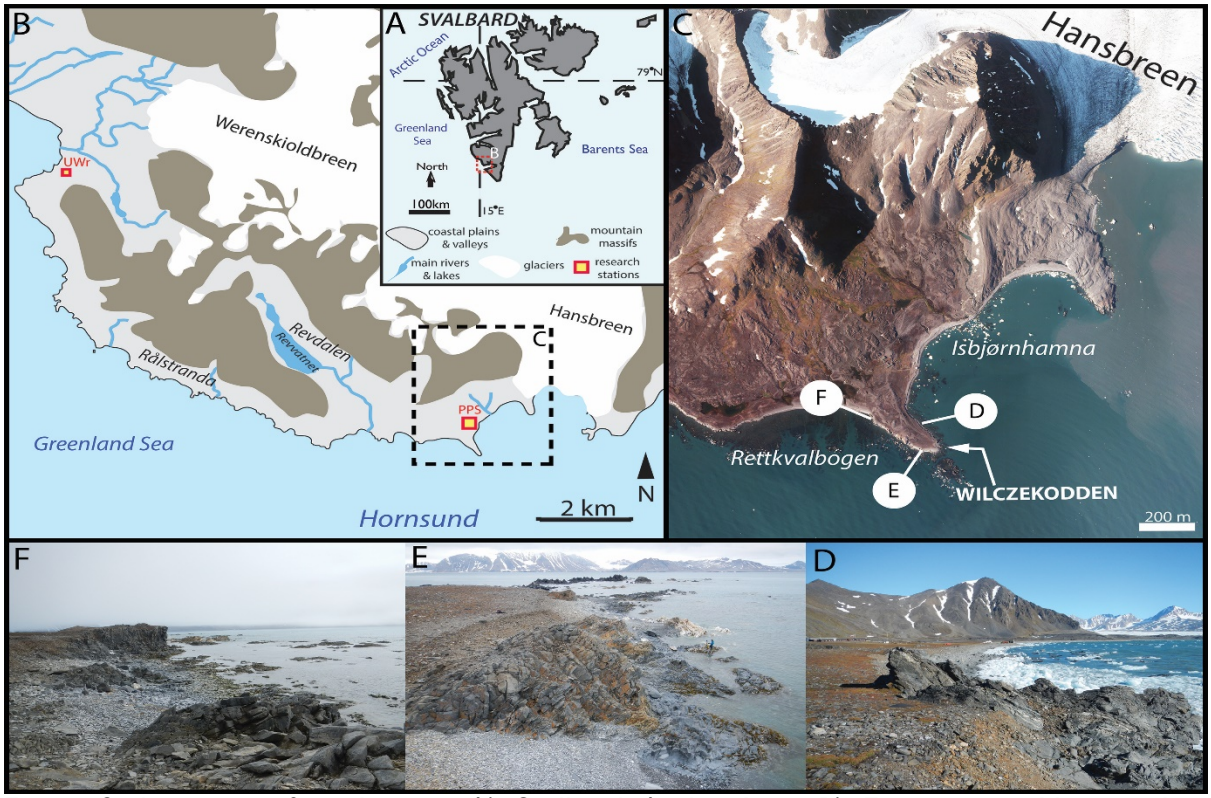

Figure 2. Location of study area A) Svalbard Archipelago; B) Entrance to Hornsund in southwestern part of Spitsbergen, largest island of Svalbard Archipelago; C) Wilczekodden – rocky cape near Polish Polar Station. Background aerial image taken by Norwegian Polar Institute in 2011; D) Eastern coast of Wilczekodden composed of shale. Cliff base, shore platforms and skerries are frequently impacted by icebergs and growlers resulting from calving of tidewater Hansbreen; E) Tip of Wilczekodden with well-developed shale and marble shore platforms, exposed to storm waves arriving from Greenland Sea; F) high cliffs and wide platforms along western coast of Wlczekodden.

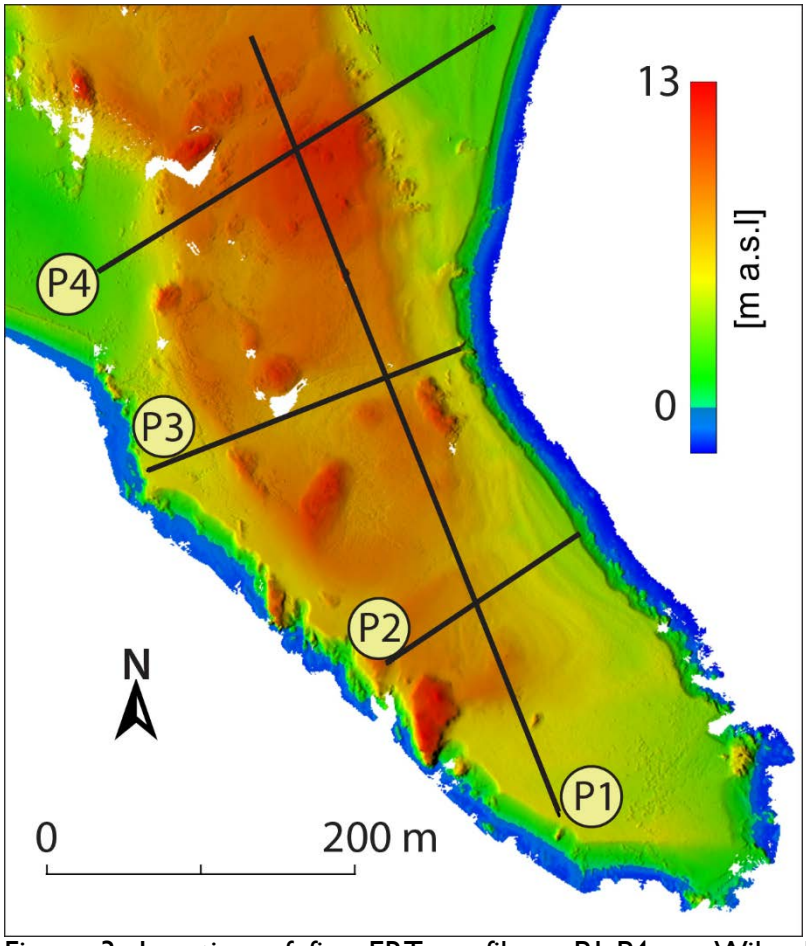

Figure 3. Location of five ERT profiles : P1-P4 on Wilczekodden. Background – Digital Elevation Model based on terrestrial laser scanning in years 2015-2016.

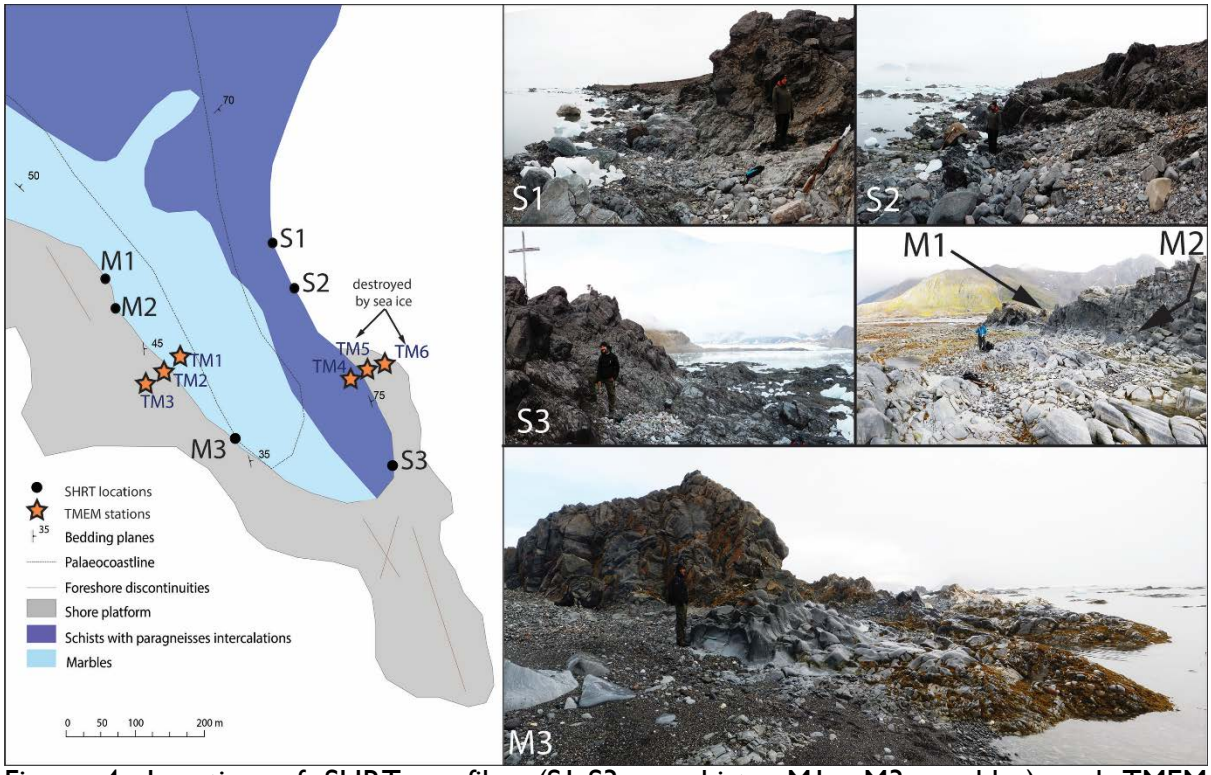

Figure 4. Location of SHRT profiles (S1-S3 – schists; M1 –M3 marbles) and TMEM measurements sites (TM1-TM6). Background geological map of the study area modified from Czerny et al. (1992a).

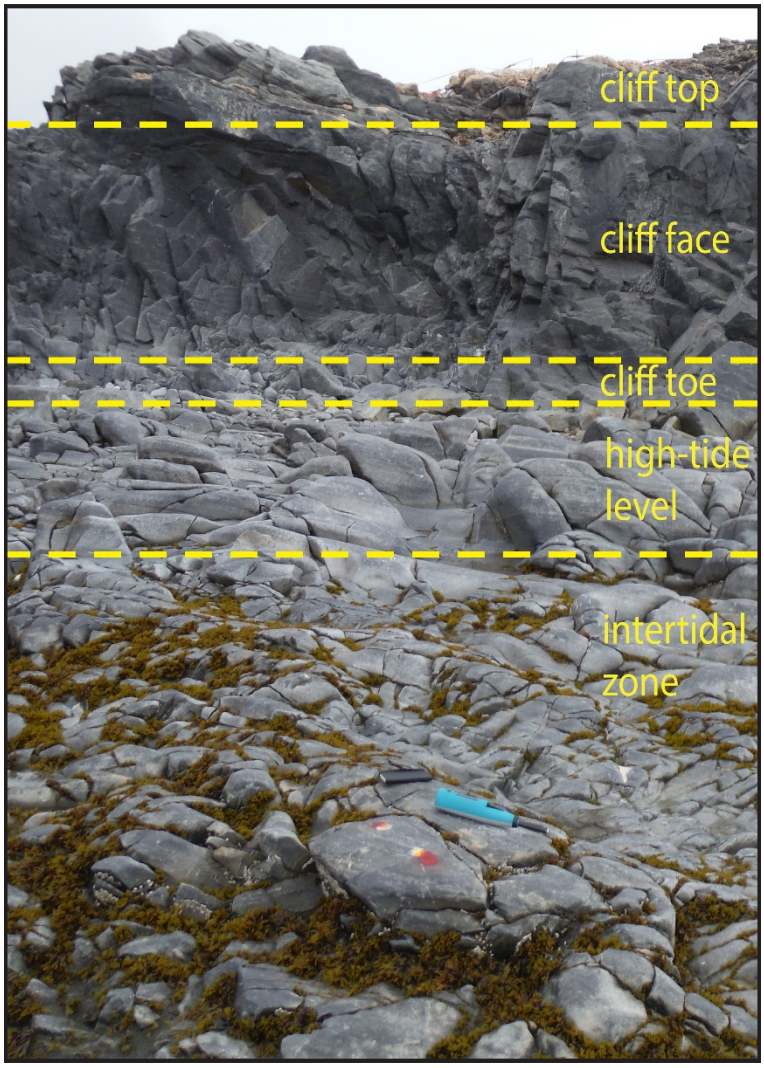

Figure 5. Five zones across the rocky shore profile from which SHRT measurements were acquired. The photograph was taken at location M2 (author: Heather Bell, Durham University).

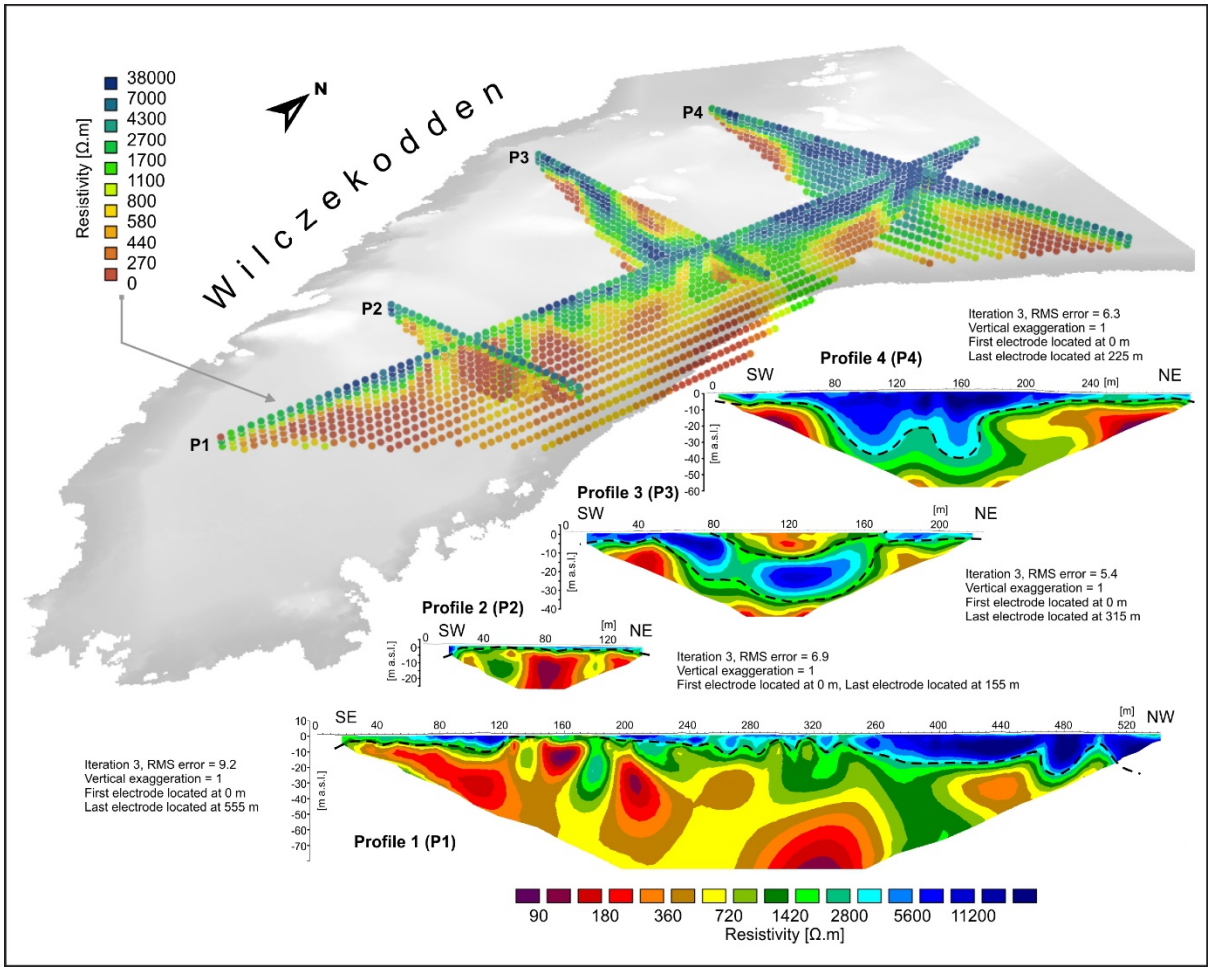

Figure 6. Results of electrical resistivity tomography on Wilczekodden. Obtained inversion models (profiles P1–P4), imaging apparent resistivity of ground, are presented separately and as oblique view in combination with digital terrain model (greys). High values of resistivity (blue colours marked also by dotted lines) are interpreted as frozen ground.

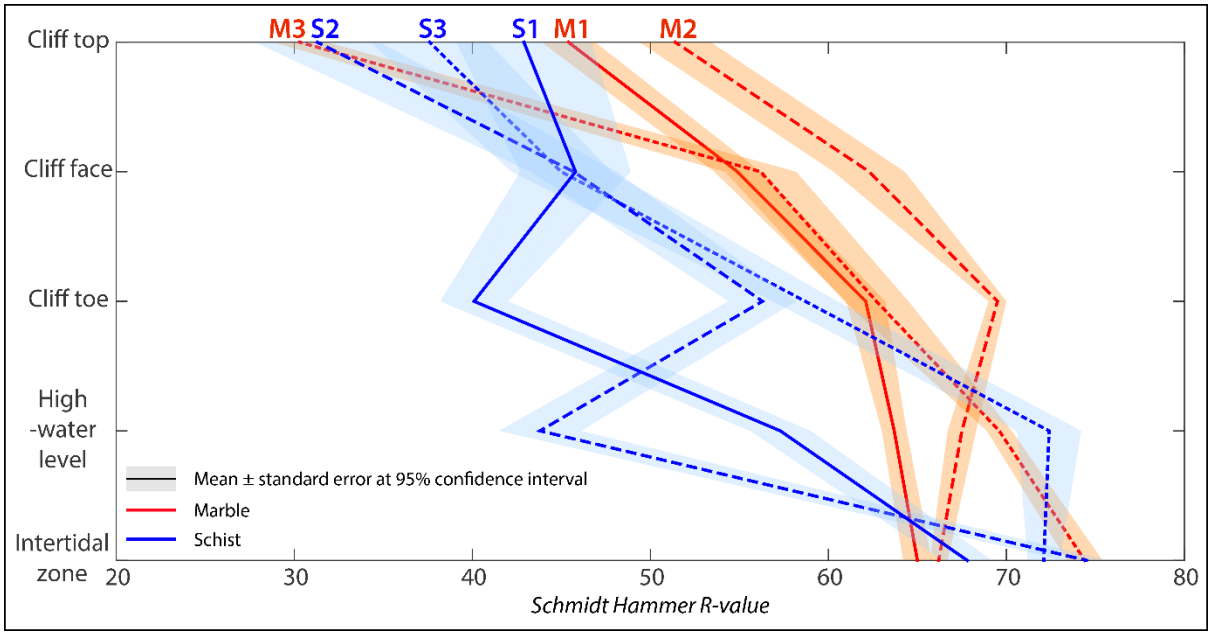

Figure 7. Schmidt hammer R-values at different elevational zones for six locations along the coast of Wilczekodden, Hornsund, Svalbard.

Figure 8. Surface change rates observed in three TMEM stations installed across marble rock coast, between 2nd of August 2015 and 21st of July 2016.

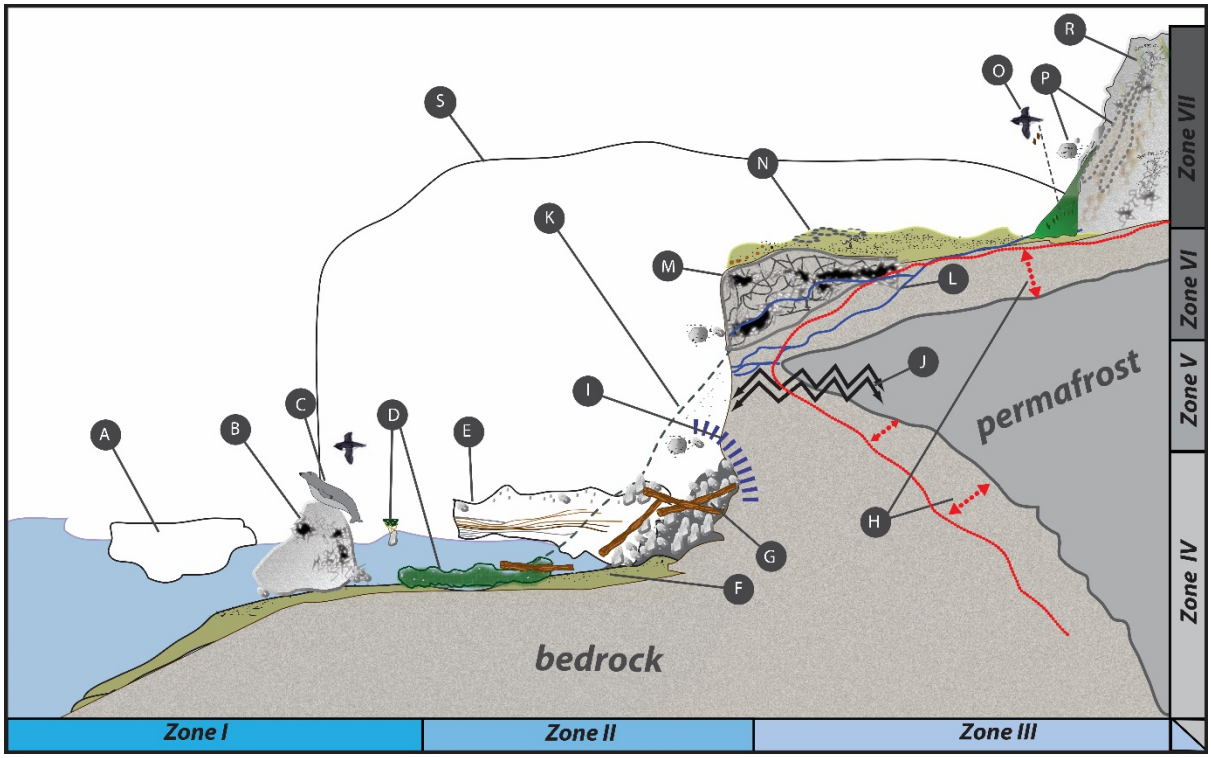

Figure 9 . Environmental factors controlling the functioning of High Arctic rock coasts: A - sea ice action; B - glacial erratics/ boulders accumulations in the intertidal zone; C - bioerosion/weathering of rock fragments in the intertidal zone; D - sediment transport and protection by seaweeds; E- development of icefoot complex; F-accumulation/redistribution of sediment cover on shore platforms; G- accumulations of driftwood, H – active layer development including bottom active layer postulated by Kasprzak et al.(2016), I - upper limit of storm wave action and sea spray extent, J - postglacial rock debuttresing, K - snowdrift/avalanche derived deposits, L – groundwater and springs, M - karstic landforms and processes (rock dependent) , N – uplifted marine deposits with various degrees of periglacial sorting; O - vegetated slopes (fertilized by bird colonies). P- debris flows and rockfalls; R - relict/uplifted rock coasts (cliffs and platforms). Zones I – VII refer to Table 1.

750 Table 1. Zonation of a High Arctic rock coast system based on mechanism controlling coastal zone development

High Arctic rock coast zone	Mechanisms
Zone I	● Seaward section of shore-platform, exposed during the low spring tides, subject to sea ice scouring and deposition of drop stones, affected by thermal changes in subsea permafrost.
Zone II	● Landward section of the shore platform, in summer months subject to tidal-dependent wetting-drying cycle as well as to operation of waves that redistribute sand-gravel sediments on the platform surface. The thickness, size and roundness of sediment covering the shore platform influence the efficiency of wave quarrying and the rate of rock surface polishing. Wave and tidal action is also responsible for driftwood and seaweed accumulations within the zone, which may have an impact on shore platform microrelief (Strzelecki, 2016). The degree of rock saturation is dependent on the development of an active layer which in this zone often occurs in a discontinuous form (e.g. Kasprzak et al., 2016). Saturated, often cracked rock surfaces are prone to disintegration due to freeze-thaw cycles. In winter, this zone is protected by an icefoot complex and thick snowdrifts (Strzelecki, 2016).
Zone III	● Inner part of the rocky outcrop bounded by permafrost and affected by post-glacial debuttressing after retreat of glacier/ice stream filling the fjord during glaciation; potential to evolve into a new shore platform.
Zone IV	● Section covering the junction with the modern shore platform and cliff wall. Affected by tides, waves and sea spray with very diverse microrelief and often covered with halokarstic features (dependent on rock lithology). Subject to intensive wetting-drying during open-water months and intensive frost weathering during cooler months. Protected by icefoot complex and thick snowdrifts in winter (e.g. Jahn, 1961; Ødegård and Sollid, 1993; Ødegård et al., 1995);
Zone V	● Middle zone of the rockwall, which is not reached by waves and sea spray, affected by thermal changes in the permafrost bounding the inner section of outcrop and post-glacial rock debuttresing (e.g. Wangensteen et al., 2007; Strzelecki, 2011). Rock shelves within this zone are often covered with debris. Summer thawing of active layer opens the network of karstic channels which often progress down the rockwall (Strzelecki, 2016). In winter months this zone is protected by sporadic snowdrifts.
Zone VI	● Top of the rocky cliff is often characterized by heavily weathered rock layers related to lack of the snow insulation and intensive biochemical weathering (particularly around bird colonies) as well as periglacial weathering (e.g. Strzelecki, 2011; Strzelecki, 2016). Often covered with uplifted marine deposits and debris/rock falls from surrounding talus slopes, drift-mantled slopes and mountain slopes (e.g. Kasprzak et al., 2016).
Zone VII	● Section of relict cliffs and shore platforms currently reshaped by operation of periglacial and paraglacial geomorphic processes (e.g. Migoń, 1997).

751

752
753